■ 2342

The Research on Telemetry Modulation System

Wu Guo-Hui*, Dai Ji-Yang, Chu Bao-Jun
Nondestructive Text Key Laboratory of Ministry Education,Nanchang Hangkong University
Nanchang Jiangxi,330063, China
*Corresponding author, e-mail: 43151481@qq.com

Abstract

To develop the effective aerospace telemetry communication system, for aerospace telemetry communication requirements high-speed, high bandwidth, high efficiency and low interference, puts forward the C-WQPSK (C-W Quadrate Phase- Shift Keying) modulation method. This method based on direct carrier QPSK, didn't consider base band pulse signal, and redesigned the modulating waveform, its phase angle jump and jump to change duration time all can be changed. Also it gives the C-WQPSK performance and theory analysis, and with QPSK, FQPSK the performance comparison, Through the MATLAB simulation experiment, verify this modulation method is correctness and effectiveness.

Keywords: telemetry, modulation system, FQPSK, C-W Quadrature phase- shift keying

1. Introduction

PCM-FM modulation system, due to good anti-interference performance, not only is the United States communication standard-IRIG standard recommended the main telemetry system, but also widely used in international aerospace telemetry communication. But this system low bandwidth utilization efficiency, Spectrum roll down slowly, easy to interfere with its adjacent channel signal communication, such as GPS, etc. In recent years, along with the missile and other aerospace vehicle rapid development, remote transmission rate has been by dozens of KBPS development to 8 MBPS even higher, aerospace vehicle test increasingly frequent, frequency band resources increasingly nervous, therefore a lot of international scholars engaged in high bandwidth efficiency digital modulation method research, Such as BPSK, QPSK and its various improvement system, etc. These modulation mode envelope constant, high power spectrum efficiency, But because of its spectrum side lobe roller drop speed slow, high band external energy. In the aerospace communication produce spectrum extension chance greatly increase [1,2]. High bandwidth utilization efficiency and high rate transmission characteristics, as a kind of remote sensing standard modulation system write in IRIG 106-2000 standard, and expected to replace PCM-FM modulation system in the future, become IRIG the main telemetry system.

But, as a kind of military telemetry standards, due to the United States patent protection, against in the international promotion and use, so the paper is based on telemetry communication system advantage[3..10], developed a kind of autonomous modulation mode C-WQPSK, It directly use N cycles of sine and reverse wave,respectively corresponding sine wave signal +1 and -1, based on direct carrier QPSK, didn't consider baseband pulse signal, redesigned the modulating waveform, its phase angle jump and jump to change duration time all can be changed. Thus has the advantages of side lobe roll down quick. Adjacent-channel interference small,etc.

2. QPSK, FQPSK, C-WQPSK Modulation Principle and Performance Analysis

2.1. QPSK Modulation Principle and Performance Analysis

Digital phase modulation (PSK) refers to the use of carrier phase change to deliver digital information, and at the same time amplitude and frequency remain unchanged [11]. QPSK is quaternary phase-shift keying signal, is a kind of digital modulation mode. The mathematical is shown in Eq. 1

$$S_{QPSK}(t) = \sum_{k=-\infty}^{\infty} g(t-kT)\cos(w_c t + \varphi_k)$$

$$= \sum_{k=-\infty}^{\infty} a_k g(t-kT)\cos w_c t - \sum_{k=-\infty}^{\infty} b_k g(t-kT)\sin w_c t \qquad (1)$$

QPSK modulator principle, is made up of two BPSK modulator. Input serial binary signal sequence, Series/parallel transformation, which respectively produce double polarity level signal $I(t)$ and $Q(t)$, and then respectively use and-modulation, add together after, its QPSK signal is shown in Figure 1
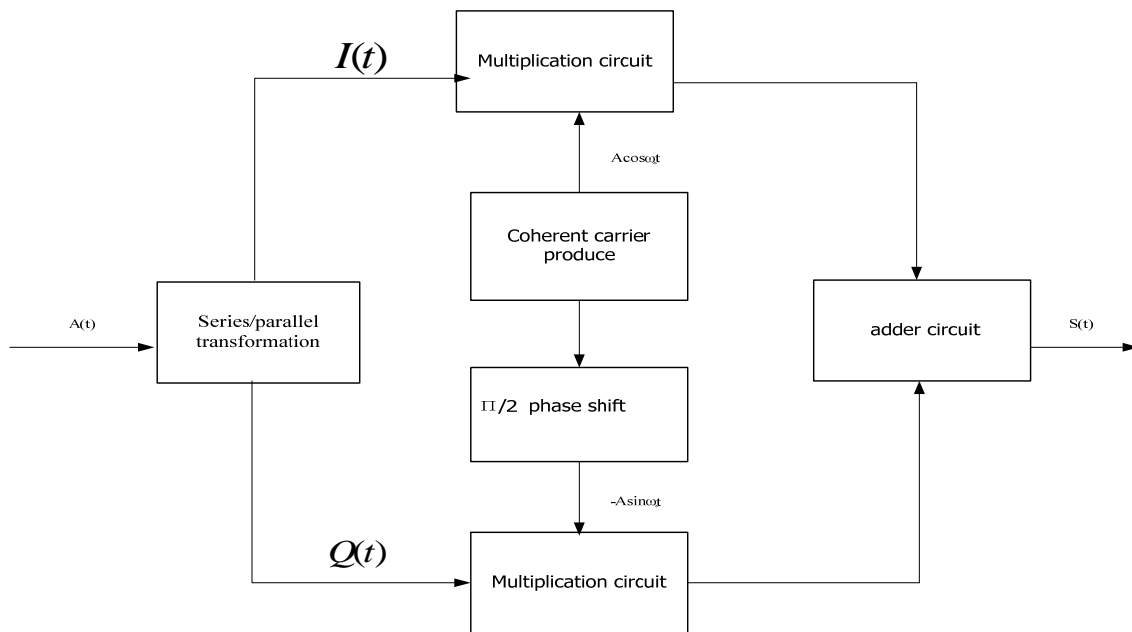

Figure 1. QPSK orthogonal modulation block diagram

QPSK modulation signal power spectrum density shown in Eq. 2

$$S_{QPSK}(f) = PT_s (\frac{\sin \pi f T_s}{\pi f T_s})^2 \qquad (2)$$

In the Eq. 2, P is sending power, T_s is symbol interval. Progressive roller drop speed of power spectral density with f^2 changed, where $f=1/T_s=1/(2T_b)$, its first zero (main lobe width) appeared.

When system using coherent demodulation, QPSK signal error rate shown in Eq. 3

$$P_e = 1-[1-\frac{1}{2}erfc\sqrt{r/2}]^2 \qquad (3)$$

In the Eq.2, r is signal-to-noise ratio.

2.2. FQPSK Modulation Principle and Performance Analysis

In the FQPSK modulation, processing modulation signal is based on IJF-OQPSK signal [12]. Behind IJF coding increased cross correlation arithmetic unit, in order to reduce its envelope of fluctuate. Modulation diagram as shown in Figure 2.
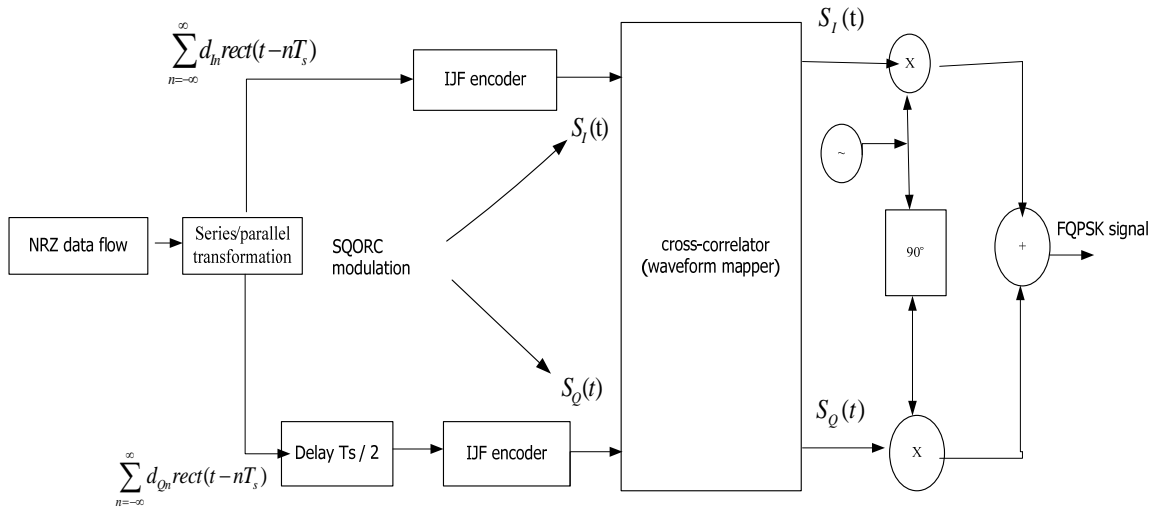
Figure 2. FQPSK modulation block diagram

The enhanced FQPSK in each full symbol interval, directly on the I and Q input data sequence on a map. In the each channel arbitrary transmitting interval, I and Q wave choice depends on the channel in the recent data jump and another channel in recent two successive data jump, this marks the FQPSK is a memory modulation method, can be described as Eq. 4.

$$s_0(t) = A, -\frac{T_s}{2} \le t \le \frac{T_s}{2} \qquad\qquad s_8(t) = -s_0(t)$$

$$s_1(t) = \begin{cases} A, -\dfrac{T_s}{2} \le t \le 0 \\ 1-(1-A)\cos^2\dfrac{\pi t}{T_s}, 0 \le t \le \dfrac{T_s}{2} \end{cases} \qquad s_9(t) = -s_1(t)$$

$$s_2(t) = \begin{cases} 1-(1-A)\cos^2\dfrac{\pi t}{T_s}, -\dfrac{T_s}{2} \le t \le 0 \\ A, 0 \le t \le \dfrac{T_s}{2} \end{cases} \qquad s_{10}(t) = -s_2(t)$$

$$s_3(t) = 1-(1-A)\cos^2\frac{\pi t}{T_s}, -\frac{T_s}{2} \le t \le \frac{T_s}{2} \qquad s_{11}(t) = -s_3(t)$$

$$s_4(t) = \begin{cases} \sin\dfrac{\pi t}{T_s} + (1-A)\sin^2\dfrac{\pi t}{T_s}, -\dfrac{T_s}{2} \le t \le 0 \\ \sin\dfrac{\pi t}{T_s} - (1-A)\sin^2\dfrac{\pi t}{T_s}, 0 \le t \le \dfrac{T_s}{2} \end{cases} \qquad s_{12}(t) = -s_4(t) \qquad (4)$$

$$s_5(t) = \begin{cases} \sin\dfrac{\pi t}{T_s} + (1-A)\sin^2\dfrac{\pi t}{T_s}, -\dfrac{T_s}{2} \le t \le 0 \\ \sin\dfrac{\pi t}{T_s}, 0 \le t \le \dfrac{T_s}{2} \end{cases} \qquad s_{13}(t) = -s_5(t)$$

$$s_6(t) = \begin{cases} \sin\dfrac{\pi t}{T_s}, -\dfrac{T_s}{2} \le t \le 0 \\ \sin\dfrac{\pi t}{T_s} - (1-A)\sin^2\dfrac{\pi t}{T_s}, 0 \le t \le \dfrac{T_s}{2} \end{cases} \qquad s_{14}(t) = -s_6(t)$$

$$s_7(t) = \sin\frac{\pi t}{T_s}, -\frac{T_s}{2} \le t \le \frac{T_s}{2} \qquad s_{15}(t) = -s_7(t)$$

For the I and Q mapping with I and Q data (0, 1) notation described as:

$$D_{In} = \frac{1-d_{In}}{2}, \quad D_{Qn} = \frac{1-d_{Qn}}{2}$$

Both the value within the (0,1). Then, define index *i* and *j* of BCD expressed as:

$$i = I_3 \times 2^3 + I_2 \times 2^2 + I_1 \times 2^1 + I_0 \times 2^0$$

$$j = Q_3 \times 2^3 + Q_2 \times 2^2 + Q_1 \times 2^1 + Q_0 \times 2^0$$

Among them:

$$I_0 = D_{Qn} \oplus D_{Q,n-1} \qquad Q_0 = D_{I,n+1} \oplus D_{In}$$

$$I_1 = D_{Q,n-1} \oplus D_{Q,n-2} \qquad Q_1 = D_{In} \oplus D_{I,n-1} = I_2$$

$$I_2 = D_{In} \oplus D_{I,n-1} \qquad Q_2 = D_{Qn} \oplus D_{Q,n-1} = I_0$$

$$I_3 = D_{In} \qquad\qquad , \qquad Q_3 = D_{Qn}$$

Can get:

$$y_I(t) = s_i(t - nT_s) \quad , \quad y_Q(t) = s_j(t - (n+1/2)T_s) \tag{5}$$

I channel and *Q* channel baseband signal respectively from 16 signal set, *I* = 0, 1,…,15 select. The implementation plan was shown in Figure 3.
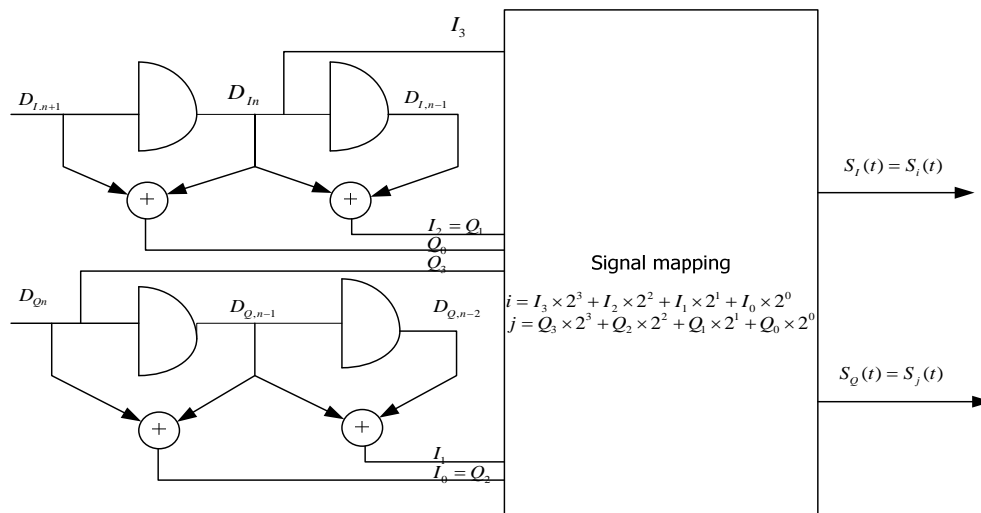

Figure 3. FQPSK modulation principle block diagram

2.3. C-WQPSK Modulation Principle and Performance Analysis

$g_0(t)$ and $g_1(t)$ respectively express send logic "*1*" and "*0*"; in the interval of [0, *Ts*], the in phase modulation output waveform is shown in Eq. 6.

$$g_1(t) = \begin{cases} \sin(w_c t + \theta), 0 \leq t < \tau, 0 \leq \theta \leq \pi \\ \sin w_c t, \tau \leq t < T_s \end{cases} \quad g_0(t) = \sin w_c t, 0 \leq t < T_s \tag{6}$$

Note that carrier angular frequency is w_c, *θ is* defined as modulation Angle or Jump to change Angle, *τ* is jump to change duration time. τ/T_s is defined as modulation duty rate, *θ* and τ common composition the modulation index of C-WQPSK. If modulation information "*1*"use the probability *P*,"*0*" use the probability *1-P*.and input Markova sequence {x_n}, Corresponding waveform is Sin(t)(0<t<Ts). there Ts is every code element transmission time. $p_i=p(x_n=i)$, $a_{ij}^k=p(x_{n+k}=j|x_n=i)$.

$$s_{x_n}(t - nT_s) = \begin{cases} g_1(t - nT_s), x_n = 1, p \\ g_0(t - nT_s), x_n = 0, 1 - p \end{cases} \tag{7}$$

The output in-phase modulated waveform is shown in Eq. 8.

$$s_I(t) = \sum_n s_{x_n}(t - nT_s) \tag{8}$$

$g_2(t)$ and $g_3(t)$ respectively express send logic *"1"* and *"0"*, in the interval of *[0,Ts]*, the orthogonal modulation output waveform is shown in Eq. 9, Eq. 10 and Eq. 11.

$$g_2(t) = \begin{cases} \cos(w_c t + \theta), 0 \le t < \tau, 0 \le \theta \le \pi \\ \cos w_c t, \tau \le t < T_s \end{cases} \quad g_3(t) = \cos w_c t, 0 \le t < T_s \tag{9}$$

$$s_{y_n}(t - nT_s) = \begin{cases} g_2(t - nT_s), x_n = 1, p \\ g_3(t - nT_s), x_n = 0, 1 - p \end{cases} \tag{10}$$

$$s_Q(t) = \sum_n s_{y_n}(t - nT_s) \tag{11}$$

Modulation waveform of C-WQPSK is shown in Eq. 12.

$$S(t) = s_I(t) + s_Q(t) = \sum_n (s_{x_n}(t - nT_s) + s_{y_n}(t - nT_s)) \tag{12}$$

The power spectrum is modulated by C-WQPSK, if sending the Markova sequence, can get the in-phase power spectrum of C-WQPSK is shown in Eq. 13.

$$P(f) = \frac{1}{8\pi^2} \cdot \frac{f_s}{(f_c^2 - f^2)^2} \sum_{n=-\infty}^{\infty} f_s \{(1 - \cos 2\pi f \tau)[f_c^2(1 - \cos\theta)^2 + f^2 \sin^2\theta]$$
$$+ f(1 - \cos 2\pi f \tau)\sin\theta]\}\delta(f - nf_c) + 2f_c \sin 2\pi fT[f_c(1 - \sin 2\pi f \tau(1 - \cos\theta)) \tag{13}$$

The power spectrum of C-WQPSK is shown in Eq. 14.

$$P_{EQPSK}(f) = \frac{1}{4\pi^2} \cdot \frac{f_s}{(f_c^2 - f^2)^2} \sum_{n=-\infty}^{\infty} f_s \{(1 - \cos 2\pi f \tau)[f_c^2(1 - \cos\theta)^2 + f^2 \sin^2\theta]$$
$$+ 2f_c \sin 2\pi fT[f_c(1 - \sin 2\pi f \tau(1 - \cos\theta)) + f(1 - \cos 2\pi f \tau)\sin\theta]\}\delta(f - nf_c) \tag{14}$$
$$+ (1 - \cos 2\pi f \tau)[f_c^2(1 - \cos\theta)^2 + f^2 \sin^2\theta]$$

From it we can see, something about the power spectrum of C-WQPSK, the symmetrical is *f=f_c*, consists of two parts: first is linear spectrum, another is continuous spectrum and reaction the random information. C-WQPSK modulation makes the energy more concentrate. When *τ* is certain, changing *θ*, can control the spectrum distribution.

The direct carrier QPSK power spectrum Eq. 4 compared with last type: the former has no linear spectrum, only the continuous spectrum, while the C-WQPSK consists of two parts: the linear spectrum and continuous spectrum, When changed *θ*, modulation energy more focused and the ability of anti-interference more strengthen; the direct carrier QPSK slowdown for the roll down rate as f^2, the roll down rate of C-WQPSK is similar to *2f^2*, and the rate increased obviously; The lord disc width of direct carrier QPSK appeared in $f = 1/T_s = 1/(2T_b)$, the first zero appeared *inf=1/τ, τ* is the jumping in duration time , usually can adjust by themselves.

Analysis Eq. 8 and Eq. 11, C-WQPSK signal can divide into two parts.

When 0≤t＜τ,θequaled to 30^0,C-WQPSK signals defined as two parts of BPSK signals respectively in two coherent detector demodulation, while its phase of BPSK signal, the noise can be impact. Due to error rate depended on each coherent detector input SNR, under the above conditions, signals power similar to receiving signal power's *1/4*, noise power is σ_n^2, if input signal noise rate is *r*, then each demodulator input signal noise rate is *r/4*. In this situation, The signal noise rate of C-WQPSK can be similar expressed is shown in Eq. 15.

$$p_e \approx 1 - [1 - \frac{1}{4} erfc \sqrt{r/4}]^2 \tag{15}$$

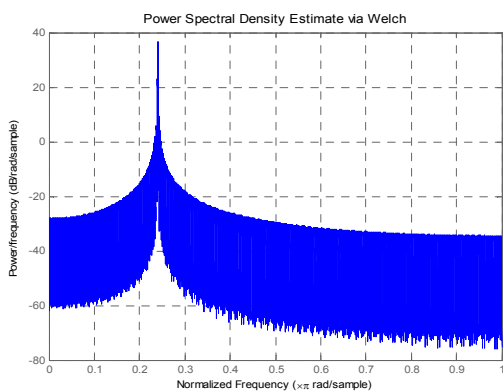When $\tau \le$ t＜T_s, the signal noise rate of C-WQPSK can be similar expressed is shown in Eq. 16.

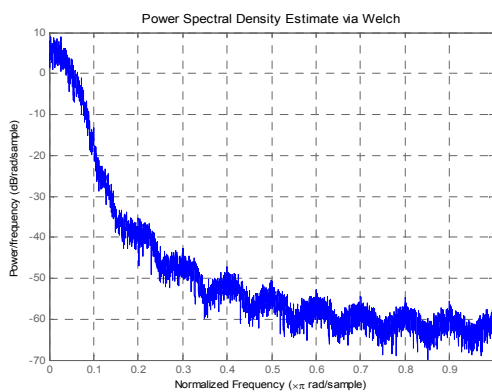$$p_e \approx 1 - [1 - \frac{1}{2} erfc \sqrt{\frac{r}{2}}]^2 \tag{16}$$

3. QPSK, FQPSK and C-WQPSK Modulation Mode Performance Simulation and Analysis
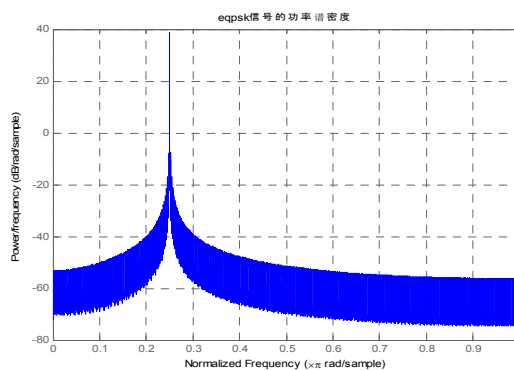### 3.1. Power Spectrum Simulation

Figure 5(a) QPSK power spectral density, figure 5(b) FQPSK power spectral density, figure 5(c) C- WQPSK power spectral density.

(a) QPSK power spectral density

(b) FQPSK power spectral density

(c) C- WQPSK power spectral density

Figure 5. Power spectral density simulation diagram

Figure 5(a), the power spectrum of QPSK from 30 db down to -30db, descend approximate 60db, but higher side lobe spectrum, high external energy, side lobe roll down slowly. Figure 5(b), the power spectrum of FQPSK from 10 db down to -65db, descend approximate 75db, low side lobe spectrum. Figure 5(c), C- WQPSK power spectrum from 38db down to -60db, descend approximate 98db, low side lobe spectrum, mezzo external energy, side lobe roll down fast.

3.2. Envelope Simulation

Figure 6(a) QPSK envelope, figure 6(b) FQPSK envelope, figure 6(c) C – WQPSK envelope.

(a) QPSK envelope

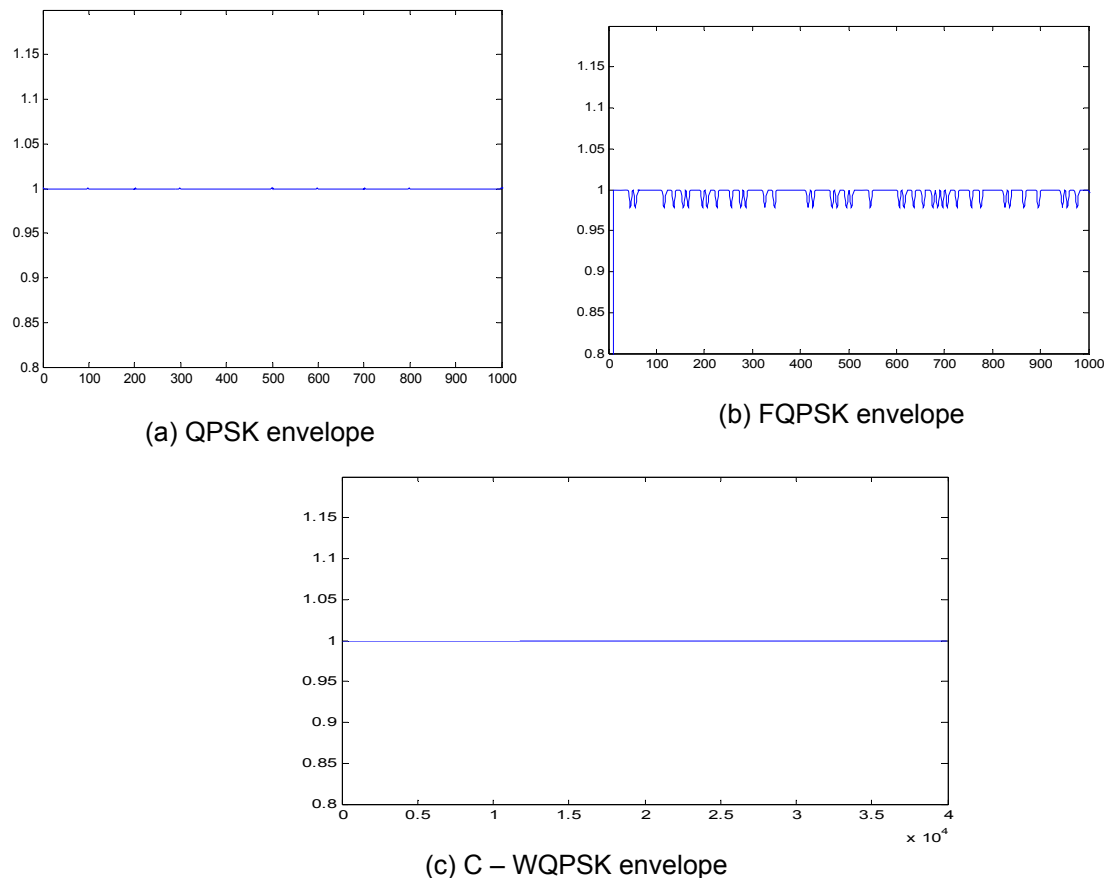(b) FQPSK envelope

(c) C – WQPSK envelope

Figure 6. Envelope simulation diagrams

Figure 6(a), the QPSK envelope fluctuation is near to zero. Figure 6(b), the FQPSK envelope fluctuation approximation is 0.18dB, figure 6(c), the C-WQPSK envelope fluctuation is zero, So C-WQPSK have constant envelope characteristic and related advantages.

3.3. Error Rate Simulation

Figure 7 FQPSK, QPSK and C-WQPSK error rate simulation. In figure 7, QPSK and C-WQPSK have the same bit error rate , when the signal-to-noise ratio is 3, the bit error rate approximate 0.2, when the signal-to-noise ratio is 10, the bit error rate approximate 0.0165. When the signal-to-noise ratio is 3, the FQPSK bit error rate approximate 0.165, when the signal-to-noise ratio is 10, the FQPSK bit error rate approximate 0.0012.

Combination above three kinds modulation mode power spectrum characteristics, envelope characteristics and error rate simulation results, we can seen that C-WQPSK has low frequency spectrum side lobe, appropriate external energy, side lobe roller drop quickly, and

constant envelope modulation advantage, compared with the other two kinds of modulation mode. But the error rate higher than FQPSK. So this modulation mode needs further improvements.
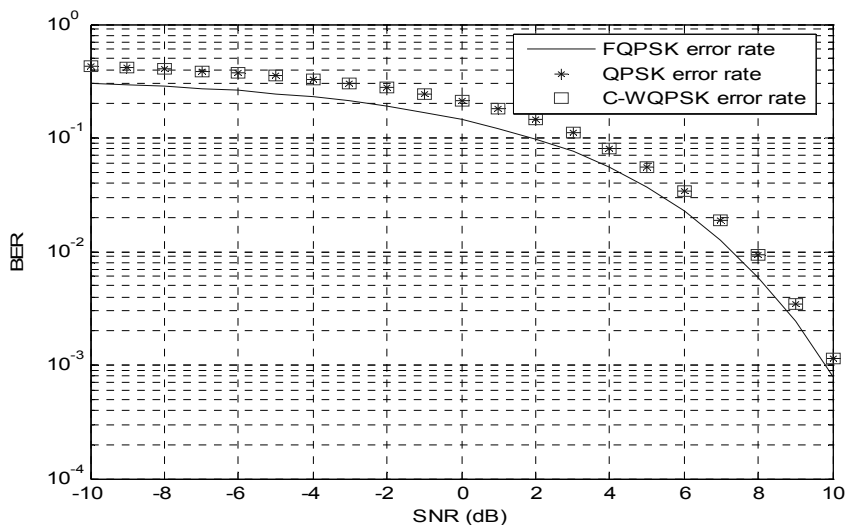

Figure 7 error rate simulations

4. Conclusion

In this paper, treat the aerospace telemetry communication modulation system related modulation method for a detailed analysis, and put forward a new modulation system C-WQPSK, with the current front aerospace modulation system FQPSK phase comparison, MATLAB simulation results show that ,this modulation has power spectrum decline rate faster, no envelope fluctuation. So can adapt to the current rapid development aerospace telemetry communication, avoid FQPSK patent disputes, Of course, compared with FQPSK, this modulation system need further improvement in the future.

References
[1] Li Hai Sheng. Satellite Communication Ultra-wideband Interference Research. *Information communication*. 2012; 1: 181.
[2] Xie Zhi Dong, Zhang Geng Xin. A Deep space Communication Constant Envelope Improved FQPSK. *Journal of Astronautics*. 2009; 30(3): 1096-1100.
[3] Zhang Si Kai, Wu Le Nan. Orthogonality and Power Spectra of EBPSK Modulated Waves. *Journal of Applied Sciences-Electronics and Information Engineering*. 2008; 26(2): 127-131.
[4] S Hoffmann, R Peveling, T Pfau, O Adamczyk, etc. Multiplier-free real-time phase tracking for coherent QPSK receivers. *IEEE Photon*. Techno Lett. 2009; 21(3): 137–139.
[5] Surinder Singh, Hari Ram, Sandeep Singh Gill. Performance Evaluation of Channel Estimation in OFDM System for Different QAM and PSK Modulations. *International Journal of Electrical and Computer Engineering*. 2011; 1(2): 140-150.
[6] Gang Yang, Jin Liu. An Algorithm for Quantitatively Calculating I/Q Gain and Phase Mismatch. *TELKOMNIKA Indonesian Journal of Electrical Engineering*. 2012; 10(4): 812-817.
[7] Kim Roberts, Kuang-Tsan Wu, Han Sun, David J, etc. Performance of Dual-Polarization QPSK for Optical Transport Systems. *IEEE, Journal of Light wave Technology*. 2009; 27(16): 3546-355.
[8] Meng Chao. Investigations on properties of (ZnO: Al) films prepared by RF/DC co-sputtering PDF. *TELKOMNIKA Indonesian Journal of Electrical Engineering*. 2012; 10(5): 947-952.
[9] Zhang Cheng, HU AiGun. A single-side band QPSK modulation scheme. *Information technology*. 2010; 12: 40-45.

[10] Zhang Shi Kai, Wu Le Nan, Modulation optimization schemes based on geometry characteristics. *Journal of Southeast University (Natural Science Edition)*. 2009; 39(4): 673-677.

[11] Fan Chang Xin, Cao LiNa. *Communication Principle*. Beijing: National Defense Industry Press. 2009; 193-200.

[12] Marvin K Simon, Xia Yun, Sun Wie. *High Bandwidth Digital Modulation and Efficiency in Deep Space Communication Application*. Beijing: Qinghua University Press. 2006; 94-124.